Journal of Computer Science

Research Article

Dengue Fever Prediction Empowered by Radial Basis Function Networks, Dynamic Mode Decomposition, and Learning-Based Foraging Algorithm

Archana T and Faritha Banu J

Department of Computer Science and Engineering, SRM Institute of Science and Technology, Ramapuram, Chennai-600089, India

Article history
Received: 11-07-2025
Revised: 12-01-2026
Accepted: 31-01-2026

Corresponding Author:
Archana T
Department of Computer Science and Engineering, SRM Institute of Science and Technology, Ramapuram, Chennai-600089, India
Email: archanat@srmist.edu.in

Abstract: Dengue fever is presently considered a major health threat that must be addressed. External and internal factors that induce nonlinear oscillations in the occurrence of dengue disease have made optimal resource allocation stimulating. Public health initiatives aimed at eradicating this vector use accurate and timely data through field processes. In dengue-endemic nations, early dengue prediction remains a main concern for public health. Developing a robust forecast model for accurate dengue prediction is a challenging task that can be accomplished through the application of a diversity of data modeling methods. Dengue fever remains a significant global public health concern, and the effort and dynamism make traditional methods challenging to predict. Combining Radial Basis Function Networks (RBFNs) with Dynamic Mode Decomposition (DMD) and Learning-Based Foraging Algorithm (LBFA), a novel method is applied for predicting dengue disease. By including RBFNs, a robust machine learning tool, the non-linear associations and patterns are extracted from dengue fever data. DMD, a data-driven decay method, enables the elucidation of the important modes and dynamics in time series data, thereby providing valuable insights into disease communication patterns. Also, LBFA, inspired by the foraging behavior of fruit flies, develops the parameters of the RBFN model, thereby improving its precision and flexibility. Using historical dengue fever data from multiple regions, inclusive tests were conducted to evaluate our proposed RBFN-DMD method. In terms of accuracy and reliability, the RBFN-DMD with LBFA outperforms predictive forecasting methods in predicting dengue fever. Additionally, our method provides interpretable insights into the driving forces and dynamics of dengue fever transmission, enabling public health establishments to make more cognizant decisions about disease prevention and control.

Keywords: Radial Basis Function Networks, Deep Learning (DL), Dynamic Mode Decomposition, Learning-Based Foraging Algorithm (LBFA)

Introduction

Dengue fever is a disease spread by mosquitoes that affects the majority of the world's tropical regions. There are three dissimilar ways that dengue can appear: Severe dengue, dengue with warning signs, and dengue without any warning signs (Sutriyawan et al., 2022). It is more typical for dengue fever to appear without warning signals, while warning indications are present in only a small percentage of cases. Dengue Hemorrhagic Fever (DHF) is a subtype of dengue that is characterized by severe symptoms and warning indications, including plasma leakage. Dengue is thought to affect between 50 and 500 million persons worldwide each year (Abualamah et al., 2021). Probably 2.5 billion people are vulnerable to infection, with a yearly human toll of 10,000–20,000 people. By 2080, 60% of people on Earth would be at risk of contracting dengue fever, according to recent estimates (Messina et al., 2019). This estimate places the number of dengue deaths at 10,000 across more than 125 countries globally. The fact that 99% of dengue-related deaths are avoidable highlights the importance of

reported cases with mortality rates above 1% globally (Othman et al., 2022).

Dengue fever, caused by the dengue virus, typically presents with a sudden high fever, severe headaches, pain behind the eyes, and joint and muscle pain (Thirugnanam and Jahir Hussain, 2023). Other common symptoms include nausea, vomiting, fatigue, and skin rashes that appear two to five days after the onset of fever. In severe cases, dengue can progress to dengue hemorrhagic fever, which is characterized by bleeding, blood plasma leakage, and potentially life-threatening low platelet count. Prompt medical attention is crucial for managing the symptoms and preventing complications (Archana and Banu Jamaly, 2023; Banu et al., 2024).

Investigating the potential of Radial Basis Function Networks in predicting dengue illness is the aim of this study. Our primary goal is to develop dependable and precise forecasting models by considering the proposal, training processes, and integration of multiple data sources. The main objective of this research is to advance data on the dynamics of dengue fever and provide healthcare authorities with an invaluable resource to develop their capability for and reaction to this complex and constantly changing public health hazard. In this study, a combination of Learning-Based Foraging Algorithm (LBFA), Dynamic Mode Decomposition (DMD), and Radial Basis Function Network (RBFN) for the dengue prediction problem was selected. This triad was chosen based on its complementary strengths in addressing the unique characteristics of dengue data. LBFA enables efficient extraction of binary and texture-level features, reducing dimensionality and eliminating irrelevant or noisy attributes from clinical and environmental datasets. DMD, on the other hand, is highly effective in capturing the underlying temporal dynamics of disease spread, especially when dealing with non-stationary and seasonally influenced time-series data. Finally, RBFN, known for its universal approximation capability and nonlinear modeling efficiency, serves as a lightweight yet powerful predictor that works well with the transformed and reduced input features provided by LBFA and DMD. The proposed LBFA-DMD-RBFN framework provides a modular, interpretable, and computationally efficient solution that addresses spatial, temporal, and predictive aspects of the dengue dataset. The experimental results demonstrate that this combination outperforms individual models or simpler alternatives in terms of prediction accuracy and generalization, thereby validating the methodological choice both theoretically and empirically.

The main contribution of the paper is:

- By utilizing RBFNs, an influential machine learning technique, this study seeks to develop a unique method for forecasting dengue infection. Non-linear relations and patterns in dengue fever data are discovered by integrating RBFNs
- Data-driven decomposition techniques, such as DMD, assist in identifying the significant dynamics and modes in time series data, providing important new data on the patterns of disease transmission. Also, LBFA improves the RBFN model's parameters, increasing its resilience and precision
- Using historical dengue fever data from multiple regions, we performed complete tests to assess our proposed RBFN-DMD method. In terms of accuracy and dependability, the RBFN-DMD with LBFA outperforms conventional forecasting methods in forecasting dengue fever
- Lastly, in addition, our method proposes interpretable insights into the driving forces and dynamics of dengue fever transmission, allowing public health establishments to make more informed decisions concerning disease prevention and control

Literature Review

Salim et al. (2021) analyzed dengue incidence prediction models in Malaysia using various machine learning techniques. Among them, the Support Vector Machine (SVM) with a linear kernel achieved the best results with 70% accuracy, 95% specificity, and 56% precision, highlighting week-of-year as the key determinant of dengue outbreaks. Similarly, (Balamurugan et al., 2020) proposed the Entropy Weighted Score-based Optimal Ranking Algorithm (EWSORA) to enhance feature selection and classification performance. Using real-time laboratory test records from Tamil Nadu, the study demonstrated improved model accuracy in identifying significant features contributing to dengue infection.

These studies indicate that traditional ML algorithms can effectively capture dengue-related patterns, though their ability to learn temporal and nonlinear relationships remains limited.

Doni and Sasipraba (2020) developed an LSTM-RNN model to predict dengue cases in India, achieving 89% infection rate accuracy and 81% mortality prediction accuracy. Similarly, Xu et al. (2019) used an LSTM-based framework in China, obtaining RMSE values between 12.99 and 24.91%, outperforming other models by predicting dengue incidence up to one month in advance.

Bogado et al. (2021) extended this by clustering LSTM models for 217 Paraguayan cities, integrating climate and weekly dengue incidence data. The approach improved prediction accuracy by 31.6% in low-incidence cities.

These deep learning studies demonstrate LSTM's effectiveness in capturing temporal dependencies, yet they often lack optimization for high-dimensional and noisy datasets.

Shaikh et al. (2023) designed an Optimized Ensemble Classifier (OEC) using the Neighbour Count–based Dragonfly Electric Fish Optimization (NC-DEFO) algorithm for feature selection, combining CNN, ANN, and SVM models. The system not only predicted dengue but also suggested preventive and treatment measures. Mussumeci and Codeço (2020) employed Random Forest regression with multivariate time-series predictors to improve regional dengue forecasting in Brazil, capturing both spatial and temporal variations. Hoyos et al. (2023) introduced federated learning frameworks based on fuzzy cognitive maps for mortality prediction and clinical decision support in severe dengue cases from Colombia. This decentralized model improved efficiency and privacy preservation. Jin et al. (2022) proposed a hybrid ARIMA–LSTM model to forecast COVID-19 predictions. The ARIMA component effectively captured the linear temporal trends in the epidemiological time series, while the LSTM network modeled complex nonlinear dependencies and long-term temporal correlations.

These hybrid approaches enhance performance through feature optimization, ensemble modeling, and federated learning, but often remain computationally intensive.

Unlike the above studies, which focus on either temporal modeling or feature optimization, our proposed model integrates temporal dynamics, spatial features, and optimization-based learning within a unified architecture. This combination enables more accurate and interpretable dengue prediction while addressing issues of overfitting, data imbalance, and generalization across diverse regions.

Limitations of the Existing System

- Most existing dengue forecasting models are built on aggregated population-level data, lacking the ability to personalize predictions based on individual health characteristics such as age, comorbidities, or genetic susceptibility
- Human mobility patterns, including personal travel and regional migration, are rarely incorporated into predictive frameworks, even though they significantly affect dengue transmission dynamics
- Many models do not account for individual behavioral factors, such as the use of mosquito repellents, hygiene practices, and adherence to public health guidelines, limiting the real-world applicability of their predictions
- The variability in access to healthcare services and differences in reporting accuracy can lead to biased datasets, which the existing systems fail to adjust for, reducing the reliability of the predictions
- Existing systems often adopt static modeling approaches and do not dynamically adapt to personal or environmental changes over time, leading to a lack of responsiveness in rapidly changing epidemiological contexts

Materials and Methods

This section offers a new technique to predict dengue disease by assimilating Radial Basis Function Network (RBFNs), a robust machine learning tool to extract non-linear correlations and patterns from dengue fever data. DMD, a data-driven decomposition method, simplifies the clarification of the underlying modes and dynamics in time series data, thereby providing valuable insights into disease transmission patterns. Additionally, LBFA, Learning-Based Foraging Algorithm, improves the RBFN model's parameters, increasing its pliability and precision. This algorithm is inspired by the foraging behavior of fruit flies. In terms of accuracy and dependability, the RBFN-DMD with LBFA outperforms conventional forecasting methods in predicting dengue fever. Figure 1 shows the block diagram of the proposed method.

Dataset

The dataset used for this study was obtained from Kaggle. It comprises anonymized clinical and environmental records covering multiple regions of South Asia. For the purpose of dengue prediction and severity analysis, only dengue-specific records were extracted, resulting in a refined dataset focused on confirmed dengue and non-dengue cases. The dataset features patient demographics (age, gender), clinical indicators (temperature, platelet count, WBC count, symptoms), and environmental variables (humidity, rainfall, temperature). This dataset was selected for its diversity and relevance to dengue epidemiological factors. To address class imbalance, the Synthetic Minority Oversampling Technique (SMOTE) was applied, followed by validation to maintain feature distribution consistency and avoid synthetic bias.

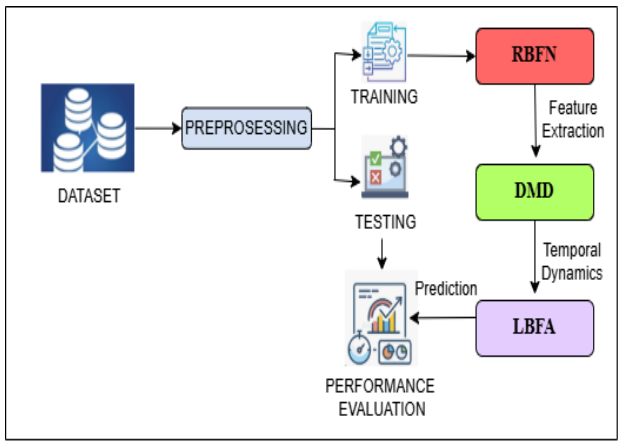

Fig. 1: Architecture diagram of the proposed method

The primary goal of this dataset is to enable physicians to perform tasks and apply knowledge to the field of medical science. The CSV file has 74 columns in total. Individual symptoms are signified by the first 64 columns and clinical reports by the next 9 columns, and the prognosis is shown by the final column.

Training and Testing

Two categories are created from the data: Training data and testing data. Testing data is utilized for optimization, and training data is used for developing the model. An 80: 20% ratio is used to allocate data for testing and training. To further guarantee the resilience and variability of the model, 5-fold cross-validation is used (Anggraeni et al., 2024).

Data Pre-Processing

Numerous data difficulties, such as noise, missing values, incorrectly labeled data, excessive dimensionality, and unequal class distribution, can arise from the vast amounts of medical data collected from diverse sources. The pre-processing stage in this proposed study addresses the imbalanced data by utilizing the Symmetric Minority over-Sampling Technique (SMOTE) (Ning et al., 2018). The performance of several traditional classifiers in classification is improved by this application. As such, the outcomes obtained using this method perform better than those obtained using a dataset that is balanced. Using the following formula, instances for the balanced dataset are produced:

$$(B'_{new1}, B'_{new2}) = (B_{11}, B_{12}) + Rand(0-1) * (B_{new1}, B_{new2}) \quad (1)$$

Where:

$$B_{new1} = B_{21} = B_{11} \; and \; B_{new2} = B_{22} - B_{12}$$

According to Eq.1, the initial attribute value of the first instance is represented by B11, the first attribute value of the second instance is denoted by B21, the closest attribute value of the first instance (in the second position) is labelled as B12, and the closest attribute value of the second instance (in the second position) is indicated as B22. The random number ranging from 0 to 1 is included in Rand (0–1). After pre-processing, the dataset balance is tested using correlation-based feature selection (CFS), genetic algorithms (GA), and particle swarm optimization (PSO) to determine whether SMOTE affected the initially unbalanced dataset.

Radial Basis Function Networks

A common kernel function in many kernelized learning techniques is the RBF neural network. There are three main layers in a radial basis function neural network: The input layer, the hidden layer using a non-linear RBF activation function, and the output layer, which is linear. The RBF neural network's development and effective mapping from $Z^z \rightarrow Z^s$ are demonstrated in Figure 2.

Each and every input connects to every hidden neuron (neural unit). This suggests that the activation function of the hidden neuron is a radial basis function, and as a result of factorability, the Gaussian function is frequently chosen over other radial basis functions. Consequently, it is common to assume that the radial basis function is Gaussian and that the Euclidean distance serves as the norm. Neuronal activation decreases with increasing distance from the radial basis function centre of a neuron's input. The radial basis function using the input vector $y_q \in Z^z$ can be written as:

$$Z(y_q - d_i) = exp\left(-\frac{1}{2\sigma^2}\|y_q - d_i\|^2\right) \quad (2)$$

Where Q is the sample count and $y_q = (y_1^q, y_2^q, \ldots, y_m^q)^T$ is the entire number of examples. T is the q-th term's input sample; $\| y_q - D_i \|$ represents the Euclidean norm; D_i and σ correspond to the center and variance of the Gaussian function, respectively. After that, the output of the network is shown as follows:

$$X_j = \sum_{i=1}^{h} \omega_{ij} \exp\left(-\frac{1}{2\sigma^2} \| y_q - D_i \|^2\right) \quad (3)$$

The statement represents the network's actual output, X_j, which originates from the j-th node linked to the input example. It includes the number of neurons $i = 1, 2, 3, \ldots, h$ in the hidden layer, as well as the weight of the connection ω_{ij} that connects the hidden layer to the output layer.

The confirmation of the odd function's variance occurs when the expected result of the sample is [18]:

$$\sigma = \frac{1}{Q} \sum_j^m \| C_j - X_i d_i \|^2 \quad (4)$$

The formulation of the Radial Basis Function (RBF) learning technique is given in the subsequent text.

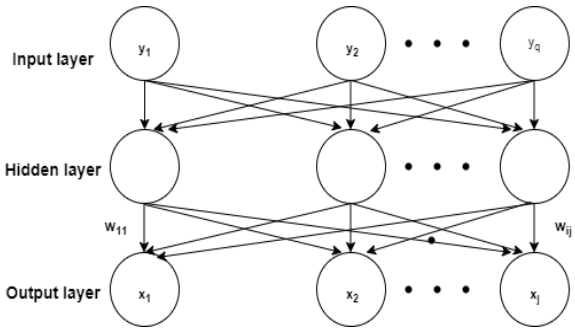

Fig. 2: Radial Basis Function Networks Architecture

Step 1: To find the basis function at the center, K-means clustering is used.

Initializing the network: A random selection is made from a set of h training samples to determine the centre of the Gaussian function, or the central point for clustering in d_i.

By calculating the Euclidean distance between the mean d_i and y_q, the closest neighbour approach is used to assign the training examples to each clustering class:

$$\vartheta_q \ (q = 1, 2, 3, \ldots . Q)$$

Modifying the clustering centre. Within each clustering class, ϑ_q or the new clustering center, the mean value for the training sample is computed. d_i takes over the radial basis function's central location if the new state doesn't change. If not, move on to step 2 and perform a new calculation.

Step 2: Determine the Gaussian function σ_i variance.

The following expression satisfies the Gaussian function σ_i variance requirement:

$$\sigma_i = \frac{D_{max}}{\sqrt{2h}} \ i = 1, 2, \ldots, h \tag{5}$$

Within each set of di, d_{max} is the maximum Euclidean distance.

Step 3: Determining the neural unit's strength of connection among the hidden and output layers, as provided by:

$$\omega = \exp\left(\frac{h}{D_{max}^2} \parallel y_q - d_i \parallel^2\right) \ i = 1, 2, \ldots . , h; \tag{6}$$

$$q = 1, 2, \ldots \ldots , Q$$

Dynamic Mode Decomposition

The Koopman operator, initially introduced in the field of fluid mechanics, serves as the foundation of DMD. The eigenmodes of an approximate linear model are typically computed using this method. In this context, the Dynamic Mode Decomposition (DMD) is described through the lens of matrix decomposition. This viewpoint establishes the foundation for the future investigation of low-rank and sparse decomposition in the following section.

The matrix $Y \in R^{NX\,M}$ can be used to depict the image series:

$$Y = [Y_1, Y_2, \ldots \ldots , Y_N] \tag{7}$$

This indicates the i^{-th} image with the vector $Y \in R^{NX\,1}$. For us, the series of M images represents a rough linear model.

A Koopman operator $B \in R^{NX\,N}$ is assumed to link the i-th snapshot to the following (i + 1)-th snapshot, which is:

$$y_{i+1} = B_{yi} + Z_i \tag{8}$$

The residual vector is represented by $Z_i \in R^{NX\,1}$. In the following ways, matrices can be created from the data:

$$Y_d = [Y_1, Y_2, \ldots \ldots , Y_{M-1}] \tag{9}$$

$$Y_d = [Y_1, Y_2, \ldots \ldots , Y_{M-1}] \tag{10}$$

Eq. 8,9,10 allow us to derive Eq.11:

$$Y_q = BY_d + Z \tag{11}$$

Alternatively, consider a case where the (i + 1) images cover a linear space. Accordingly, the $(i+1)^{-th}$ image in this case can be approximately reflected by a linear combination of the preceding images:

$$y_M = \alpha_1 y_1 + \alpha_2 y_2 + \cdots . + \alpha_{M-1} y_{M-1} + q \tag{12}$$

The residual vector is denoted by $q \in R^{NX1}$.

Eq. 12 then has the following form:

$$y_M = Y_d \alpha + q \tag{13}$$

Where $\alpha = [\ \alpha_1, \alpha_2, \ldots \ldots . . \alpha_{M-1}]^T$. Thus, Y_q can be expressed as follows:

$$Y_q = Y_d U + q e_{M-1}^T \tag{14}$$

Where the $(M-1)^{-th}$ unit vector is denoted by e_{M-1}, and the companion matrix $U \in R^{(M-1)X(M-1)}$ is found by:

$$U = \begin{bmatrix} 0\,0 & \ldots & 0\,\alpha_1 \\ 1\,0 & \ddots & \vdots\ \ \alpha_2 \\ 0\,1 & \ddots & 0\ \ \vdots \\ \vdots \ddots & \ddots & 0\,\alpha_{M-2} \\ 0 & \ldots & 0\,1\ \ \alpha_{M-1} \end{bmatrix} \tag{15}$$

After $Y_d = RQ$ indicates the RQ-decomposition of Y_d, Equation (13) least squares solution for α can be found by:

$$\alpha = Q^{-1} R^H y_M \tag{16}$$

Since the linear approximation model allows us to ignore the residuals in Equations (11) and (14), we obtain:

$$BY_d = Y_d U \quad (17)$$

The eigenvalues and eigenvectors of B are actually more important than the matrix itself. Therefore, the eigenvalue and singular value decompositions are used to lower the computational complexity. If $Y_d = K\Sigma V^H$ represents Y_d singular value decomposition, then:

$$B = K\tilde{U}K^{-1} \quad (18)$$

Where:

$$\tilde{U} = \sum V^H U(\sum V^H)^{-1} \quad (19)$$

The eigenvalue problem can be resolved by:

$$\tilde{U}W_i = \lambda_i W_i \quad (20)$$

Where λ_i is the $\tilde{U}$ $i^{\text{-th}}$ eigenvalue, and W_i is the eigenvector corresponding to it. Equation (18) can be expressed as follows:

$$B = KW\Delta W^{-1}K^{-1} \quad (21)$$

Where W is the matrix whose columns contain W_i and Δ is the diagonal matrix with λ_i, the diagonal component.

The eigenmodes of an approximate linear model are the subject of research in the science of fluid mechanics. It is possible to depict the eigenmodes using the eigenvalues and eigenvectors of B. Instead, it is more interesting in how the eigenmodes express Y. Consequently, additional work has been conducted (Yin et al., 2018).

Any column of Y can be expressed as follows by omitting the residuals:

$$y_i = B^{i-1}y_1 \quad (22)$$

Once $\Phi = KW$is defined, $\Phi^{-1} = K^{-1}W^{-1}$. Once b is defined as $a = \Phi^{-1}{}_{y1}$, any column in Y can be expressed as follows:

$$y_i = \Phi\Delta^{i-1}a \quad (23)$$

If T is solved by $a = [a_1, a_2, \ldots\ldots\ldots a_k]^T$ if $i = 1. a = (\Phi^H\Phi)^{-1}\Phi_{y1}$, where k is the number of non-zero eigenvalues corresponding to B.

Eq. 23 can be written as follows since Δ^{i-1} is a diagonal matrix:

$$y_i = \Phi \begin{bmatrix} a_1 & 0 & \ldots & 0 \\ 0 & a_2 & \vdots & \\ \vdots & \ddots & 0 & \\ 0 & \ldots & 0 & a_k \end{bmatrix} \begin{bmatrix} \lambda_1^{i-1} \\ \lambda_2^{i-1} \\ \vdots \\ \lambda_k^{i-1} \end{bmatrix} \quad (24)$$

Therefore:

$$Y = \Phi AV_{and} \quad (25)$$

In this case, A is a diagonal matrix with diagonal elements indicated by a_i, while V_{and} stands for the Vandermonde matrix:

$$V_{and} = \begin{bmatrix} 1 & \lambda_1 & \ldots & \lambda_1^{M-1} \\ 1 & \lambda_2 & & \lambda_2^{M-1} \\ & \vdots & \ddots & \vdots \\ 1 & \lambda_k & \ldots & \lambda_k^{M-1} \end{bmatrix} \quad (26)$$

Now, using the eigenvalues and eigenvectors of B, Y is expressed as the product of three matrices. In the following part, it will be applied to sparse and low-rank decomposition.

Learning-Based Foraging Algorithm (LBFA)

Learning-Based Foraging Algorithm can be used for dengue prediction in several ways.

Optimizing Predictive Models: The algorithm can optimize the parameters of machine learning models used for dengue prediction, such as regression models, decision trees, or neural networks, by efficiently searching through the parameter space to find the most accurate settings.

Feature Selection: It can identify and select the most relevant features from datasets related to dengue outbreaks, such as climate conditions, historical cases, and socio-economic factors, improving the model's performance by focusing on the most impactful variables.

Pattern Recognition: The algorithm can assist in discovering patterns and correlations within the data that are indicative of dengue outbreaks, helping to build more robust and accurate predictive models.

Data Preprocessing: It can optimize data preprocessing steps, such as handling missing values or scaling features, to enhance the quality of the input data used in predictive models.

By integrating machine learning techniques with the foraging-inspired search process, this approach can improve the accuracy and efficiency of dengue prediction models, leading to better forecasting and timely public health interventions.

Fruit flies have exceptional olfactory and visual abilities, using both their sense of smell and their eyesight to locate food and other members of their species. Fruit flies use their acute sense of smell to select the strongest aroma when seeking food. As a result, their motions are guided by visual signals as they use their vision to recognize both food sources and other flies (Shi et al., 2020).

Using a broad definition, the following can be used

to express the basic difficulty in obtaining global optimization inside the continuous domain:

$$s.t.\, y_j^{\min R(y)} \in [Y_{min}, Y_{max}], j = 1,2,3, \ldots M \quad (27)$$

When using the M-dimensional choice variable $y = (y_1, y_2, \ldots, y_M)$, the objective function is represented by $R(y)$, and the decision space's lower and upper bounds are indicated by y_{min} and y_{max}, respectively.

The maximum iteration count (NZ) and the population size represented by C_{pop} are two of the FOA features. Random initialization establishes the initial position of the (y_{best}, X_{best}) fruit fly swarm in the decision space. Using a broad definition, the following can be used to express the basic difficulty in obtaining global optimization inside the continuous domain.

Olfactory Intelligence

This uses the intelligence of AI and advanced technologies in interpreting and utilizing olfactory data. The fruit fly swarm develops a total of C_{pop} new sites for the food source using a random mechanism. By using its olfactory intelligence mechanism, the swarm disperses these spots at random throughout its current location:

$$\begin{Bmatrix} y_i = y_{best} + rand(-1,1) \\ x_i = x_{best} + rand(-1,1) \end{Bmatrix} \quad (28)$$

Here, the coordinates of the i-th fruit fly are indicated by y_i and X_i, and a random number selected from the interval (-1, 1) is represented by $i = 1, 2, \ldots, C_{pop}$.

There is a scent concentration judgment linked to every place created throughout the olfactory intelligence process. As you recognize, the K_i is the reciprocal of the length between the starting point and the destination:

$$\begin{bmatrix} M_i = \sqrt{y_i^2 + x_i^2} \\ K_i = 1/M_i \end{bmatrix} \quad (29)$$

The fragrance concentration evaluation K_i is connected with $R(.)$ in the FOA framework, and it serves as a potential solution for the objective function in the decision space:

$$smell_i = R(K_i) \quad (30)$$

Cognitive Vision

The use of artificial intelligence to enhance visual search by mimicking human cognitive processes enables advanced perception, recognition, and interpretation of visual data. This approach combines AI with visual analytics to achieve human-like understanding and decision-making. The fruit fly swarm uses this mechanism for greedy selection. It chooses the optimal spot with the least amount of fragrance concentration after examining each site that the previous olfactory intelligence produced:

$$Index = \arg\min (smell_i) \quad (31)$$

First, the optimal fragrance concentration $smell_{index}$ produced by olfactory intelligence with the scent concentration $smell_{best}$ at the y_{best}, X_{best} is compared. If $smell_{index} < smell_{best}$, the fly swarm uses visual search to find its new position (y_{index}, X_{index}), which takes the place of the previous position y_{best}, X_{best}. This procedure clarifies how the visual search works.

$$\begin{cases} y_{best} = y_{index} \\ X_{best} = X_{index} \end{cases}$$
$$\text{if } smell_{index} < smell_{best}$$
$$smell_{best} = smell_{index} \quad (32)$$

The scent and vision search processes are conducted repeatedly until something happens that triggers the program to end. Algorithm 1 outlines the general procedure used by the FOA to solve the minimum problem R(y).

Algorithm 1 LBFA Process

//Initialization
Set the population size C_{pop} and the max number of iterations NZ.
Initialize the fruit fly swarm's location, (y_{best}, x_{best}), in the search space, randomly.
//Iterative Search
for n=1: NZ
//Olfactory Intelligence
for i=1: C_{pop}
$y_i = y_{best} + rand(-1,1)$
$x_i = x_{best} + rand(-1,1)$
//Calculate the smell concentration
$M_i = \sqrt{\{y_i^2 + x_i^2\}}$
$K_i = \frac{1}{M_i}$
$smell_i = R(K_i)$
end for
// Cognitive Visual
Index = argmin($smell_i$)
if $smell_{index}$ is less than $smell_{best}$ of the fruit fly swarm's location (y_{best}, x_{best})
then
Fruit flies move to the location (y_{index}, x_{index}) and update the smell concentration:
$y_{best} = y_{index}$
$x_{best} = x_{index}$
$smell_{best} = smell_{index}$
end if
end for

Table 1 lists the various mathematical symbols used in the RBFN-DMD and LBFA methods.

Table 1: Description of mathematical symbols

Symbol	Description
$y_q \in \backslash \mathbb{R}^r$	input vector
Q	total number of
$\|\| y_q - D_i \|\|$	Euclidean norm
$\boldsymbol{C}$	sample's intended
σ_i	Gaussian function
$Y \in R^{NX\,M}$	image series
$Y_t \in R^{NX\,1}$	i-th snapshot
$z_i \in R^{NX\,1}$	residual vector
$U \in R^{(M-1)X(M-1)}$	companion matrix
Δ	diagonal matrix
V_{and}	Vandermonde matrix
A	diagonal matrix
a_i	diagonal elements
R(y)	objective function
(NZ)	maximum number of
C_{pop}	population size
$smell_{best}$	smell concentration
(y_{best}, x_{best})	original fruit fly swarm
M	Dimensional

Results and Discussion

The experimental setup is covered in the results section, followed by a description of the performance metrics and an analysis of the findings. A selection of five comparative methods, EWSORA, KTEAED, LSTM, SVM, and ANN, was made to represent a broad spectrum of techniques commonly applied in dengue prediction and medical data analysis. EWSORA and KTEAED are included as they are advanced rule-based and embedding-based diagnostic models that offer strong performance in structured clinical data contexts. LSTM is widely recognized for its effectiveness in modeling temporal patterns, while ANN and SVM serve as well-established machine learning baselines with frequent use in healthcare prediction tasks.

Comparative Methods

Entropy Weighted Score-based Optimal Ranking Algorithm (EWSORA), Knowledge Tensor Embedding with Association Enhancement Diagnosis (KTEAED), Long Short-Term Memory (LSTM), Support Vector Machine (SVM), and Artificial Neural Network (ANN) are the current systems.

KTEAED: Knowledge Tensor Embedding with Association Enhancement Diagnosis is an AI diagnosis approach that applies matrix embeddings to detect the clinical outcomes of key data elements by identifying their links to outcome entities (Xi et al., 2022).

EWSORA: The Entropy Weighted Score-based Optimal Ranking methodology (EWSORA) is a novel approach used for feature selection in the field of medical data analysis and prediction.

LSTM: LSTM models forecast the impact of dengue by leveraging time-series data such as temperature, humidity, personal travel history, and previous health records. These networks can identify patterns and provide personalized risk assessments, enabling targeted preventive measures.

ANN: Artificial Neural Networks (ANNs) offer a potential benefit in forecasting fluctuations in the mosquito population (Lee et al., 2016).

SVM: SVM models can provide risk assessment for individuals, aiding in targeted preventive measures and healthcare interventions.

Performance Metrics

This section analyses the precision, recall, f-measure, MCC, MAE, and RMSE characteristics. False Negatives (FN) are knowledge with a positive foundation but mistakenly classified as negative. True Negatives (TN) are knowledge that is damaging and has a negative basis. Conversely, TP represents true positives and the projected amount of accurate data. Lastly, FP stands for false positives, which refers to situations in which something negative is wrongly classified as positive.

Precision is the proportion of optimistic forecasts that accurately fall into the all-positive category, as in Eq. 33:

$$\text{Prec} = \frac{\text{TP}}{\text{TP+FP}} \tag{33}$$

To calculate recall, divide the total number of positive class components by the number of True Positive (TP) results. Eq. 34 is used to determine the recall value:

$$\text{Recall} = \frac{\text{TP}}{\text{TP+FN}} \tag{34}$$

The precision and recall are averaged to produce the F1 score. Eq. 35 shows how the F1 score is determined:

$$\text{F1 Score} = \frac{2*\text{Prec}*\text{Recall}}{\text{Prec}*\text{Recall}} \tag{35}$$

Matthews Correlation Coefficient (MCC): It is a correlation coefficient of the variables that is calculated using Eq. 36:

$$\text{MCC} = \frac{\text{TP X TN} - \text{FP X FN}}{\sqrt{(\text{TP+FP})(\text{TP+FN})(\text{TN+FP})(\text{TN+FN})}} \tag{36}$$

Root Mean Square Error (RMSE): The error rate is calculated using the square of RMSE, as shown in Eq. 37:

$$\sqrt{RMSE} = \sqrt{\frac{1}{N}\sum_{i-1}^{N}(x_i - x)^2} \tag{37}$$

DOI: 10.3844/jcssp.2026.1298.1312

Precision Analysis

Table 2 compares the RBFN-DMD precision to other techniques. The graph in Figure 3 depicts that deep learning improves precision while also increasing efficiency. The precision values for the KTEAED, EWSORA, LSTM, ANN, and SVM models, for example, are 67.78, 86.45, 73.99, 91.45, and 80.98%, respectively, while the precision for the RBFN-DMD model is 95.87% for 100 data points. Nevertheless, the RBFN-DMD model has demonstrated its effectiveness across various data sizes. In this regard, the precision for RBFN-DMD with 600 data is 98.88%, whereas for KTEAED, EWSORA, LSTM, ANN, and SVM, the corresponding precisions are 72.99, 90.45, 79.99, 94.12, and 85.21%, respectively.

Recall Analysis

In Table 3, the recall of the RBFN-DMD methodology is compared to that of other methodologies. The graph in Figure 4 demonstrates how deep learning improves recall while remaining efficient. The recall values for the KTEAED, EWSORA, LSTM, ANN, and SVM models, for example, are 72.87, 80.45, 76.23, 88.33, and 85.12%, respectively, while the recall for the RBFN-DMD model is 92.77% for 100 data points. Nevertheless, the RBFN-DMD model has demonstrated its effectiveness across various data sizes. In this regard, the recall for RBFN-DMD with 600 data points is 97.44%, whereas for KTEAED, EWSORA, LSTM, ANN, and SVM, the corresponding recalls are 75.12, 84.12, 79.99, 91.87, and 87.99%, respectively.

Accuracy Analysis

In Table 4, the accuracy of the RBFN-DMD methodology is compared to other approaches, and Figure 5 depicts the graph where the deep learning method improves accuracy while remaining efficient.

Table 2: Precision Analysis for RBFN-DMD method

No. of the data set taken	KTEAED	EWSORA	LSTM	ANN	SVM	RBFN-DMD
100	67.78	86.45	73.99	91.45	80.98	95.87
200	68.12	87.88	75.66	91.55	80.91	96.12
300	69.99	88.45	76.12	92.45	81.66	97.88
400	70.66	89.67	77.98	93.33	82.66	97.45
500	71.56	90.99	78.45	93.44	84.55	98.12
600	72.99	90.45	79.99	94.12	85.21	98.88

Table 3: Recall Analysis for RBFN-DMD

No. of the data set taken	KTEAED	EWSORA	LSTM	ANN	SVM	RBFN-DMD
100	72.87	80.45	76.23	88.33	85.12	92.77
200	72.99	81.23	77.55	89.43	85.99	93.44
300	73.12	82.52	77.78	89.66	86.23	94.17
400	74.98	82.19	78.12	90.34	86.77	95.55
500	74.99	83.55	78.67	91.23	87.34	96.34
600	75.12	84.12	79.99	91.87	87.99	97.44

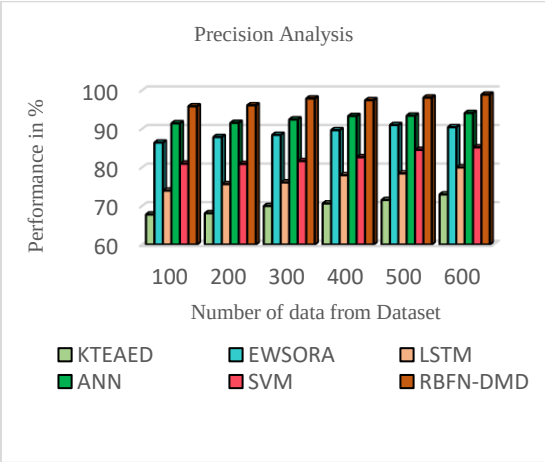

Fig. 3: Precision Analysis for RBFN-DMD

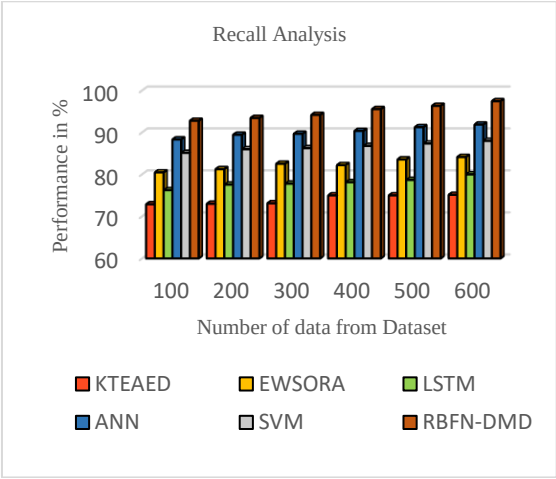

Fig. 4: Recall Analysis for RBFN-DMD

For example, the accuracy for the KTEAED, EWSORA, LSTM, ANN, and SVM models are 66.23, 72.66, 79.23, 83.67%, and 89.45%, respectively, while the RBFN-DMD model's accuracy is 91.99% for 100 data points. Nevertheless, the RBFN-DMD model has demonstrated its effectiveness across various data sizes. In this regard, the accuracy for RBFN-DMD with 600 data is 95.99%, whereas the equivalent accuracy for KTEAED, EWSORA, LSTM, ANN, and SVM is 71.34, 78.45, 82.88, 88.99, and 91.77%, respectively.

Although the proposed model achieved an accuracy of 96%, this performance is based on a controlled experimental dataset. Real-world dengue data often exhibit regional, temporal, and environmental variations that may impact prediction accuracy. Therefore, cross-validation, dropout, and early stopping were applied to mitigate overfitting, and future work will focus on testing the model across multi-regional datasets to validate its generalizability.

Table 5 presents a comparison of the effectiveness of the RBFN-DMD approach with alternative methods. The data in Figure 6 demonstrates the way the deep learning method increases efficiency. The MCC values for the KTEAED, EWSORA, LSTM, ANN, and SVM models, for example, are 70.32%, 85.21%, 75.67%, 90.99%, and 81.11%, respectively, for 100 data points. However, the RBFN-DMD model's MCC is 94.32%. Nevertheless, the RBFN-DMD model has demonstrated its effectiveness across various data sizes. In this regard, the MCC for RBFN-DMD with 600 data is 97.11%, whereas for KTEAED, EWSORA, LSTM, ANN, and SVM, the corresponding MCC values are 74.23, 89.45, 80.88, 93.88, and 84.78%, respectively.

Table 4: Accuracy Analysis for RBFN-DMD

No. of the data set taken	KTEAED	EWSORA	LSTM	ANN	SVM	RBFN-DMD
100	66.23	72.66	79.23	83.67	89.45	91.99
200	67.32	74.56	79.67	85.67	89.67	92.45
300	68.88	75.12	80.54	86.12	89.99	93.78
400	69.12	76.66	80.44	87.66	90.65	94.55
500	70.55	77.98	81.23	88.56	90.45	95.87
600	71.34	78.45	82.88	88.99	91.77	95.99

Table 5: MCC Analysis for RBFN-DMD

No. of the data set taken	KTEAED	EWSORA	LSTM	ANN	SVM	RBFN-DMD
100	70.32	85.21	75.67	90.99	81.11	94.32
200	70.99	86.67	76.23	90.45	81.56	94.67
300	71.45	87.56	77.56	91.11	82.45	95.67
400	72.78	88.56	78.12	91.89	82.78	96.34
500	73.88	89.99	79.87	92.45	83.55	96.99
600	74.23	89.45	80.88	93.88	84.78	97.11

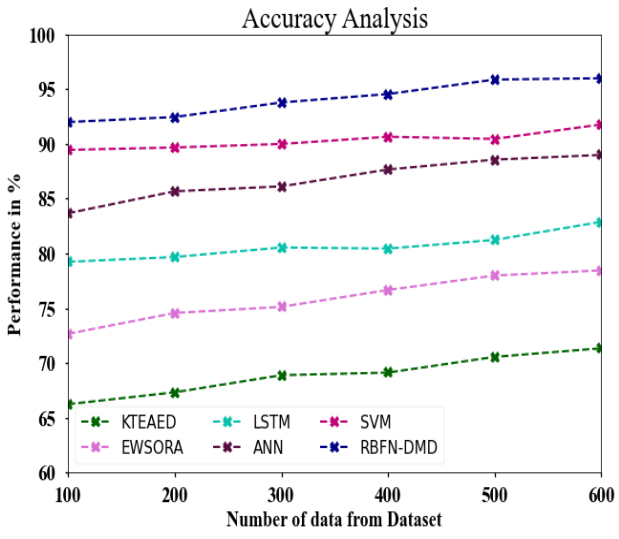

Fig. 5: Accuracy Analysis for RBFN-DMD

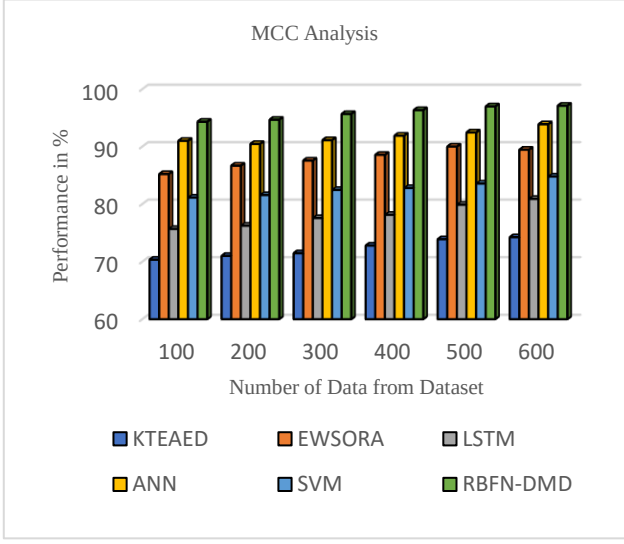

Fig. 6: MCC Analysis for RBFN-DMD

RMSE Analysis

In Table 6, an RMSE assessment of the RBFN-DMD methodology is shown in contrast to other techniques. The graph in Figure 7 illustrates that deep learning technology improves performance while maintaining a low RMSE. The RMSE values for the KTEAED, EWSORA, LSTM, ANN, and SVM models are 43.33, 38.98, 34.55, 30.12%, and 27.19%, respectively. Meanwhile, the RBFN-DMD model exhibits an RMSE of 21.65% with 100 data points. The RBFN-DMD model, however, performs best across various data, yielding low RMSE values. The RMSE value for the RBFN-DMD model with 600 data is 26.88%, whereas the KTEAED, EWSORA, LSTM, ANN, and SVM models have respective RMSE values of 48.55, 42.76, 38.56, 33.44, and 29.77%.

MAE Analysis

In Table 7, an MAE assessment of the RBFN-DMD methodology is shown in contrast to other methods. The Mean Absolute Error (MAE) measures the average magnitude of errors between predicted and actual values, without considering their direction, as shown in Figure 8. It is computed using the following Equation:

Table 6: RMSE Analysis for RBFN-DMD

No. of datasets taken	KTEAED	EWSORA	LSTM	ANN	SVM	RBFN-DMD
100	43.33	38.98	34.55	30.12	27.19	21.65
200	44.19	39.12	35.87	30.78	27.99	23.98
300	45.98	39.78	36.14	31.45	28.45	22.56
400	46.13	40.23	37.11	31.87	28.78	24.19
500	47.88	41.99	37.88	32.87	29.67	25.77
600	48.55	42.76	38.56	33.44	29.77	26.88

Table 7: MAE Analysis for RBFN-DMD

No. of datasets taken	KTEAED	EWSORA	LSTM	ANN	SVM	RBFN-DMD
100	25.16	20.67	30.55	16.56	35.18	10.56
200	26.77	20.77	30.99	17.78	36.66	11.45
300	27.78	21.13	31.11	18.23	37.77	12.59
400	28.67	22.67	32.45	18.99	39.88	13.77
500	29.11	23.98	33.67	19.56	39.77	14.76
600	29.99	24.55	34.89	19.99	40.11	15.88

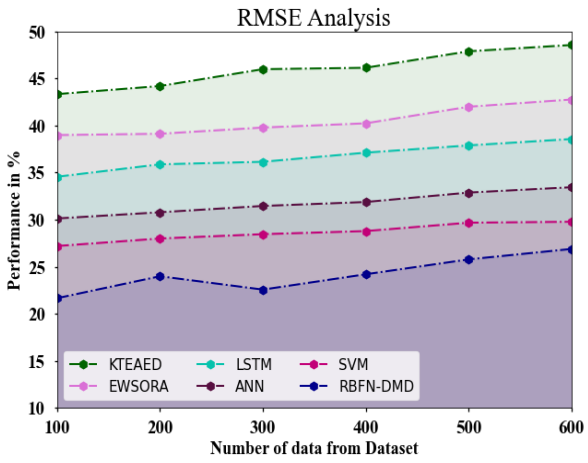

Fig. 7: RMSE Analysis for RBFN-DMD

$$MAE = \frac{1}{n}\sum_{i=1}^{n}|y_i - \hat{y}_i| \quad (38)$$

Where:

yi is the actual value
$\hat{y}_i$ is the predicted value
n is the number of observations

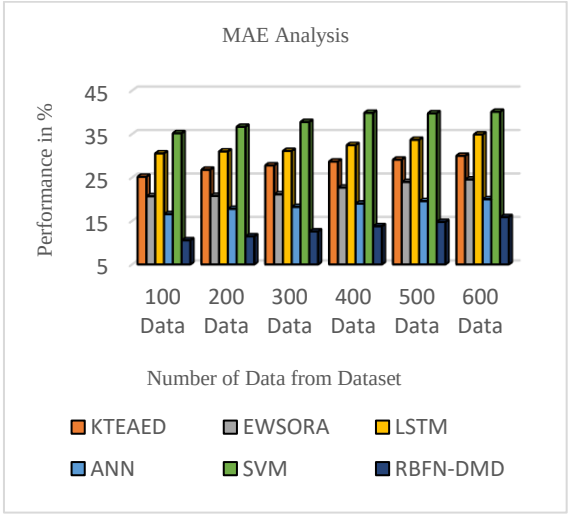

Fig. 8: MAE Analysis for RBFN-DMD

Lower MAE values indicate better predictive accuracy. The MAE values for the KTEAED, EWSORA, LSTM, ANN, and SVM models are 25.16, 20.67, 30.55, 16.56, and 35.18%, respectively. Meanwhile, the RBFN-DMD model exhibits an MAE of 10.56% with 100 data

points. The RBFN-DMD model, however, achieves the best across various datasets, yielding low MAE values. The MAE value for the RBFN-DMD model with 600 data is 15.88%, whereas the KTEAED, EWSORA, LSTM, ANN, and SVM simulations have respective MAE values of 29.99%, 24.55, 34.89, 19.99, and 40.11%.

Discussion

The RBFN-DMD method allows for the successful simulation of the intricate dynamics of dengue fever transmission. A strong foundation for disease incidence prediction was laid out by RBFNs, and significant spatiotemporal essentials could be extracted from the data with the help of DMD. With LBFA, the model parameters were fine-tuned to capture even the most nuanced changes in illness patterns, further refining the forecasting process. This hybrid methodology has the ability to help public health officials proactively manage Dengue, which can help protect vulnerable people and make the most efficient use of available resources. With the following experimental results, the proposed framework RBFN-DMD proves exceptional performance: The segmentation analysis precision is 98.88%, recall is 97.44%, f-measure is 95.99%, MCC is 97.11%, RMSE is 26.88%, and MAE is 15.88%.

Ablation Study

In the ablation study on Dengue Fever Forecasting Empowered by Radial Basis Function Networks, Dynamic Mode Decomposition, and Learning-Based Foraging Algorithm, several components were systematically removed or changed to measure their individual contributions to the forecasting model's performance. Firstly, the model was examined as a whole, including all three components. The RBFN, DMD, and LBFA were then individually removed from the model, and the forecasting accuracy was evaluated for each scenario. The results are shown in Table 8.

The study found that each vital had a considerable impact on the model's predictive powers, emphasizing their collective strength in improving the accuracy and dependability of dengue fever forecasting.

In addition to conventional models such as ANN, SVM, and LSTM, hybrid models LSTM-ANN and LSTM–ARIMA were also implemented to ensure a fair comparison with contemporary epidemic forecasting frameworks. As shown in Table 9 and Figure 9, although the hybrid model demonstrates improved accuracy of 92.56% and 93.24% over standalone LSTM and ANN models, the proposed RBFN–DMD method still outperforms it, achieving a maximum accuracy of 95.99%. This confirms the robustness of the proposed model in capturing both nonlinear and dynamic temporal relationships in dengue prediction.

In RBFN-DMD-based dengue fever forecasting, the implementation of 10-fold cross-validation (Table 10) substantially enhances model robustness and dependability. Cross-validation is a statistical methodology wherein the dataset is divided into ten segments or subsets, of which one is designated for validation, and nine are utilized for training purposes (Gupta et al., 2023).

Table 8: Ablation study of the proposed model

Model Variant	MAE	RMSE	Accuracy (%)	F1-Score
RBFN only	0.84	1.21	81.3	0.78
DMD+ RBFN	0.73	1.05	85.6	0.82
LBFA+ RBFN	0.69	0.98	86.9	0.84
LBFA+ DMD+ RBFN (Full)	0.58	0.81	90.2	0.88

The accuracy result of the proposed model achieved a superior performance of 95.99% for the input data by applying 10-fold cross-validation.

To demonstrate real-world applicability, the proposed RBFN–DMD model was evaluated using a case study based on dengue surveillance data from Tamil Nadu, India (2018-2023).

Table 9: Comparison of Accuracy Analysis for RBFN–DMD and Existing Models

Methods	Accuracy Analysis
KTEAED	71.34
EWSORA	78.45
LSTM	82.88
ANN	88.99
SVM	91.77
LSTM- RNN	92.56
LSTM-ARIMA	93.24
RBFN-DMD	95.99

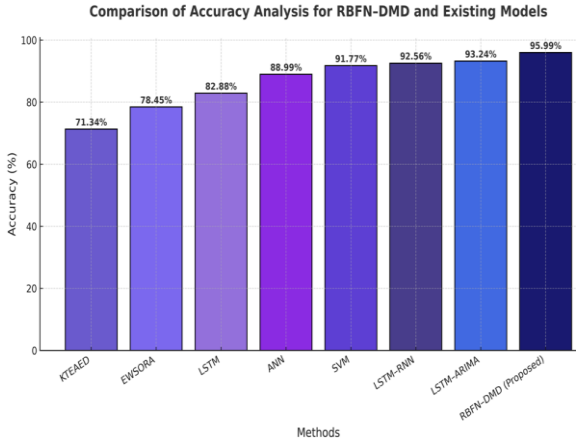

Fig. 9: Comparison of accuracy analysis for the proposed RBFN–DMD

Table 10: fold cross-validation of RBFN-DMD analysis

K-folds	RBFN-DMD Accuracy
1-Fold	0.95
2-Fold	0.96
3-Fold	0.95
4-Fold	0.95
5-Fold	0.96
6-Fold	0.97
7-Fold	0.98
8-Fold	0.98
9-Fold	0.94
10-Fold	0.95
10-Fold Mean	0.95

The dataset combined epidemiological data obtained from the National Vector Borne Disease Control Programme (NVBDCP) with environmental parameters such as temperature, rainfall, and humidity sourced from the Indian Meteorological Department (IMD). The model was deployed to forecast dengue incidence at the district level, integrating weekly climatic data. The predictions were compared with reported dengue cases to validate performance. The RBFN–DMD achieved a Mean Absolute Percentage Error (MAPE) of 4.8%, demonstrating its robustness in real data settings. This case study highlights that the proposed system offers a scalable solution for real-world implementation. It supports data-driven decision-making and proactive public health management.

Conclusion

The proposed "Dengue Fever Forecasting Empowered by Radial Basis Function Networks, Dynamic Mode Decomposition and Learning-Based Foraging Algorithm" model has shown significant results in predicting dengue fever in public health activities, with the accurate and suitable forecasts of dengue fever leading to better disease prevention and control methods. Also, combining optimization algorithms with novel machine learning methods offers a viable framework for addressing other infectious diseases and public health issues. However, the proposed RBFN–DMD–LBFA model is validated on retrospective data from limited regions of South Asia; its generalization to unseen or rapidly changing outbreak scenarios remains unverified. The DMD formulation assumes smooth temporal evolution, which may limit performance during abrupt incidence spikes. The LBFA-based optimization includes sensitivity to hyperparameter selection, which may impact model stability when extending the framework to more complex data environments. Future work will focus on validating the proposed framework using multi-regional and real-time dengue surveillance datasets to improve generalizability across diverse outbreak scenarios. In addition, Integration of domain-specific knowledge, such as expert guidelines, mosquito breeding information, mobility patterns, and vector density indicators, can also enhance epidemiological relevance and predictive stability.

Acknowledgment

Thank you to the publisher for their support in the publication of this research article. We are grateful for the resources and platform provided by the publisher, which have enabled us to share our findings with a wider audience. We appreciate the efforts of the editorial team in reviewing and editing our work, and we are thankful for the opportunity to contribute to the field of research through this publication.

Author's Contributions

Archana T: Methodology and design.
Faritha Banu J: Review and results.

Funding Information

The authors received no specific funding for this study.

Data Availability

The manuscript data set can be freely downloaded from https://www.kaggle.com/datasets.

Conflicts of Interest

The authors declare that they have no conflicts of interest to report regarding the present study.

References

Abualamah, W. A., Akbar, N. A., Banni, H. S., & Bafail, M. A. (2021). Forecasting the morbidity and mortality of dengue fever in KSA: A time series analysis (2006–2016). *Journal of Taibah University Medical Sciences*, *16*(3), 448–455. https://doi.org/10.1016/j.jtumed.2021.02.007

Anggraeni, W., Yuniarno, E. M., Rachmadi, R. F., Sumpeno, S., Pujiadi, P., Sugiyanto, S., Santoso, J., & Purnomo, M. H. (2024). A hybrid EMD-GRNN-PSO in intermittent time-series data for dengue fever forecasting. *Expert Systems with Applications*, *237*, 121438. https://doi.org/10.1016/j.eswa.2023.121438

Archana, T., & Banu Jamaly, F. (2023). Forecasting Machine Learning Based Feature Selection for Dengue Prediction in the Early Stage. *Proceeding of the 2023 3rd International Conference on Mobile Networks and Wireless Communications (ICMNWC)*, 1–6. https://doi.org/10.1109/icmnwc60182.2023.10436006

Balamurugan, S. A. alias, Mallick, M. S. M., & Chinthana, G. (2020). Improved prediction of dengue outbreak using combinatorial feature selector and classifier based on entropy weighted score based optimal ranking. *Informatics in Medicine Unlocked*, *20*, 100400. https://doi.org/10.1016/j.imu.2020.100400

Banu, J. F., Hariprasad, G., Archana, T., & Srivatsan, P. (2024). Novel Framework for Dengue Classification and Early Recovery using Machine Learning Algorithms. *Proceeding of the 2024 11th International Conference on Computing for Sustainable Global Development (INDIACom)*, 1537–1542. https://doi.org/10.23919/indiacom61295.2024.10499095

Bogado, J. V., Stalder, D. H., Schaerer, C. E., & Gomez-Guerrero, S. (2021). Time Series Clustering to Improve Dengue Cases Forecasting with Deep Learning. *Proceeding Fo the 2021 XLVII Latin American Computing Conference (CLEI)*, 1–10. https://doi.org/10.1109/clei53233.2021.9640130

Doni, A., & Sasipraba, T. (2020). LSTM-RNN Based Approach for Prediction of Dengue Cases in India. *Ingénierie Des Systèmes d Information*, *25*(3), 327–335. https://doi.org/10.18280/isi.250306

Gupta, G., Khan, S., Guleria, V., Almjally, A., Alabduallah, B. I., Siddiqui, T., Albahlal, B. M., Alajlan, S. A., & AL-subaie, M. (2023). DDPM: A Dengue Disease Prediction and Diagnosis Model Using Sentiment Analysis and Machine Learning Algorithms. *Diagnostics*, *13*(6), 1093. https://doi.org/10.3390/diagnostics13061093

Hoyos, W., Aguilar, J., & Toro, M. (2023). Federated learning approaches for fuzzy cognitive maps to support clinical decision-making in dengue. *Engineering Applications of Artificial Intelligence*, *123*, 106371. https://doi.org/10.1016/j.engappai.2023.106371

Jin, Y., Wang, R., Zhuang, X., Wang, K., Wang, H., Wang, C., & Wang, X. (2022). Prediction of COVID-19 Data Using an ARIMA-LSTM Hybrid Forecast Model. *Mathematics*, *10*(21), 4001. https://doi.org/10.3390/math10214001

Lee, K. Y., Chung, N., & Hwang, S. (2016). Application of an artificial neural network (ANN) model for predicting mosquito abundances in urban areas. *Ecological Informatics*, *36*, 172–180. https://doi.org/10.1016/j.ecoinf.2015.08.011

Messina, J. P., Brady, O. J., Golding, N., Kraemer, M. U. G., Wint, G. R. W., Ray, S. E., Pigott, D. M., Shearer, F. M., Johnson, K., Earl, L., Marczak, L. B., Shirude, S., Davis Weaver, N., Gilbert, M., Velayudhan, R., Jones, P., Jaenisch, T., Scott, T. W., Reiner, R. C., & Hay, S. I. (2019). The current and future global distribution and population at risk of dengue. *Nature Microbiology*, *4*(9), 1508–1515. https://doi.org/10.1038/s41564-019-0476-8

Mussumeci, E., & Codeço Coelho, F. (2020). Large-scale multivariate forecasting models for Dengue - LSTM versus random forest regression. *Spatial and Spatio-Temporal Epidemiology*, *35*, 100372. https://doi.org/10.1016/j.sste.2020.100372

Ning, Y., Wang, J., Han, H., Tan, X., & Liu, T. (2018). An Optimal Radial Basis Function Neural Network Enhanced Adaptive Robust Kalman Filter for GNSS/INS Integrated Systems in Complex Urban Areas. *Sensors*, *18*(9), 3091. https://doi.org/10.3390/s18093091

Othman, M., Indawati, R., Suleiman, A. A., Qomaruddin, M. B., & Sokkalingam, R. (2022). Model Forecasting Development for Dengue Fever Incidence in Surabaya City Using Time Series Analysis. *Processes*, *10*(11), 2454. https://doi.org/10.3390/pr10112454

Salim, N. A. M., Wah, Y. B., Reeves, C., Smith, M., Yaacob, W. F. W., Mudin, R. N., Dapari, R., Sapri, N. N. F. F., & Haque, U. (2021). Prediction of dengue outbreak in Selangor Malaysia using machine learning techniques. *Scientific Reports*, *11*(1), 939. https://doi.org/10.1038/s41598-020-79193-2

Shaikh, S. G., Kumar, B. S., & Narang, G. (2023). Development of optimized ensemble classifier for dengue fever prediction and recommendation system. *Biomedical Signal Processing and Control*, *85*, 104809. https://doi.org/10.1016/j.bspc.2023.104809

Shi, K., Zhang, X., & Xia, S. (2020). Multiple Swarm Fruit Fly Optimization Algorithm Based Path Planning Method for Multi-UAVs. *Applied Sciences*, *10*(8), 2822. https://doi.org/10.3390/app10082822

Sutriyawan, A., Herdianti, H., Cakranegara, P. A., Lolan, Y. P., & Sinaga, Y. (2022). Predictive Index Using Receiver Operating Characteristic and Trend Analysis of Dengue Hemorrhagic Fever Incidence. *Open Access Macedonian Journal of Medical Sciences*, *10*(E), 681–687. https://doi.org/10.3889/oamjms.2022.8975

Thirugnanam, A., & Hussain, F. B. J. (2023). Exploring Machine Learning Algorithms for the Prediction of Dengue: A Comprehensive Review. *Revue d'Intelligence Artificielle*, *37*(5), 1281–1290. https://doi.org/10.18280/ria.370521

Xi, J., Miao, Z., Liu, L., Yang, X., Zhang, W., Huang, Q., & Li, X. (2022). Knowledge tensor embedding framework with association enhancement for breast ultrasound diagnosis of limited labeled samples. *Neurocomputing*, *468*, 60–70. https://doi.org/10.1016/j.neucom.2021.10.013

Xu, J., Xu, K., & Li, Z. (2019). Developing a dengue forecast model using long short term memory neural networks method. *BioRxiv*. https://doi.org/https://doi.org/10.1101/760702

Yin, J., Liu, B., Zhu, G., & Xie, Z. (2018). Moving Target Detection Using Dynamic Mode Decomposition. *Sensors*, *18*(10), 3461. https://doi.org/10.3390/s18103461